

Journal Pre-proof

Source apportionment and health risk assessment of airborne particulates over central Indo-Gangetic Plain

Vishnu Murari, Nandita Singh, Rohit Ranjan, R.S. Singh, Tirthankar Banerjee



PII: S0045-6535(20)31338-2

DOI: <https://doi.org/10.1016/j.chemosphere.2020.127145>

Reference: CHEM 127145

To appear in: *ECSN*

Received Date: 29 February 2020

Revised Date: 27 April 2020

Accepted Date: 18 May 2020

Please cite this article as: Murari, V., Singh, N., Ranjan, R., Singh, R.S., Banerjee, T., Source apportionment and health risk assessment of airborne particulates over central Indo-Gangetic Plain, *Chemosphere* (2020), doi: <https://doi.org/10.1016/j.chemosphere.2020.127145>.

This is a PDF file of an article that has undergone enhancements after acceptance, such as the addition of a cover page and metadata, and formatting for readability, but it is not yet the definitive version of record. This version will undergo additional copyediting, typesetting and review before it is published in its final form, but we are providing this version to give early visibility of the article. Please note that, during the production process, errors may be discovered which could affect the content, and all legal disclaimers that apply to the journal pertain.

© 2020 Published by Elsevier Ltd.

Source apportionment and health risk assessment of airborne particulates over central Indo-Gangetic Plain

Vishnu Murari¹, Nandita Singh¹, Rohit Ranjan², RS Singh³ and Tirthankar Banerjee^{1,2*}

¹Institute of Environment and Sustainable Development, Banaras Hindu University, Varanasi, India

²DST-Mahamana Centre of Excellence in Climate Change Research, Banaras Hindu University, Varanasi, India

³Department of Chemical Engineering and Technology, Indian Institute of Technology (BHU), Varanasi, India

*Correspondence: tb.iesd@bhu.ac.in; tirthankaronline@gmail.com

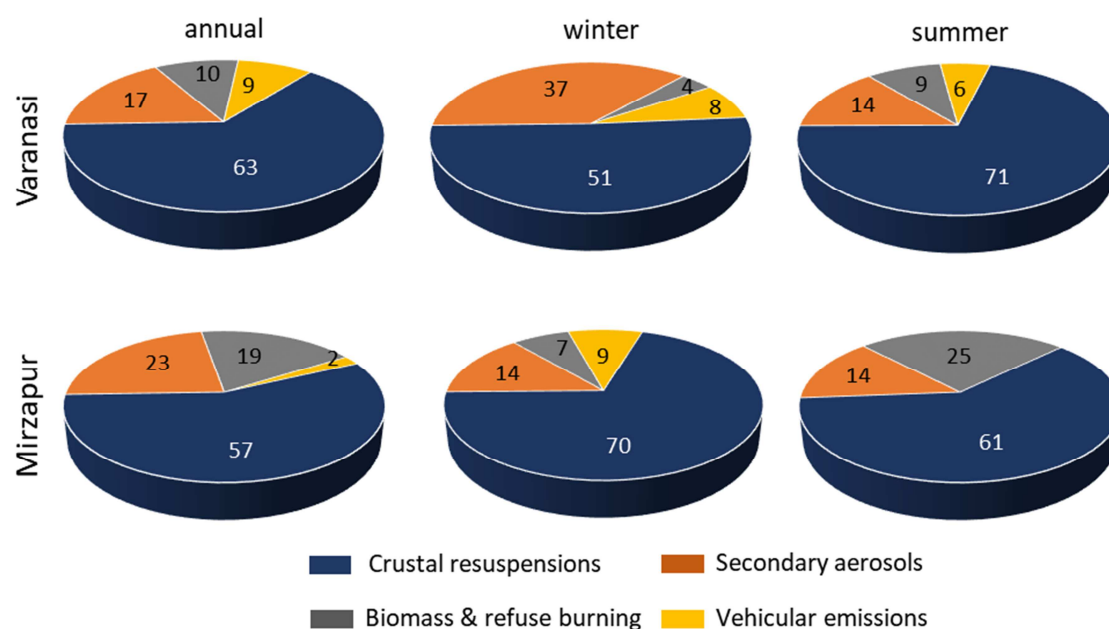
VM and TB designed the research;

VM, TB, NS, RR experimented, analyzed and interpreted the result;

TB: funding acquisition; project administration; resources; software; supervision;

NS, TB and RSS drafted the manuscript.

Graphical abstract



Relative contribution of various sources to airborne particulates.

Source apportionment and health risk assessment of airborne particulates over central Indo-Gangetic Plain

Vishnu Murari¹, Nandita Singh¹, Rohit Ranjan², RS Singh³ and Tirthankar Banerjee^{1,2*}

¹Institute of Environment and Sustainable Development, Banaras Hindu University, Varanasi, India

²DST-Mahamana Centre of Excellence in Climate Change Research, Banaras Hindu University, Varanasi, India

³Department of Chemical Engineering and Technology, Indian Institute of Technology (BHU), Varanasi, India

*Correspondence: tb.iesd@bhu.ac.in; tirthankaronline@gmail.com

Abstract

Sources of airborne particulates (PM₁₀) were investigated in two contrasting sites over central Indo-Gangetic Plain (IGP), one representing a rural background (Mirzapur) and another as an urban pollution hotspot (Varanasi). Very high PM₁₀ concentration was noted both in Varanasi (178±105µgm⁻³; N:435) and Mirzapur (131±56µgm⁻³; N:169) with 72% and 62% of monitoring days exceeded the national air quality standard, respectively. Particulate-bound elements contribute significant proportion of PM₁₀ mass (15%-18%), with highest contribution from Ca (7%-10%) and Fe (2%-3%). Besides, presence of Zn (1%-3%), K (1%-2%) and Na (1%-2%) was also noted. Water-soluble ionic species contributed 15%-19% of particulate mass, notably by the secondary inorganic aerosols (SIA). Among the SIA, sulphate (5%-7%) and nitrate (4%) were prominent, contributing 59%-62% of total ionic load, especially in winter. Particulate-bound metallic species and ions were selectively used as signatory molecules and source apportionment of PM₁₀ was done by multivariate factor analysis. UNMIX was able to extract particulate sources in both the locations and crustal resuspensions (dust/-soil) were identified as the dominant source contributing 57%-63% of PM₁₀ mass. Secondary aerosols were the second important source (17%-23%), followed by emissions from biomass/-refuse burning (10-19%). Transport of airborne particulates from upper IGP by prevailing westerly were identified as important contributor of particulates, especially during high particulate loading days. Health risks associated to particulate-bound toxic metal exposure were also assessed. Non-carcinogenic health risk was within the permissible limit while there is possibility of elevated risk for PM₁₀-bound Cr and Cd, if adequate control measures are not in place.

Keywords: Air pollution; Health risk; Heavy metals; Receptor model; UNMIX.

1. Introduction

Airborne particulates are allied to many adverse health and environmental impacts; especially in heating of lower atmosphere thereby, making changes in atmospheric thermal structure (Satheesh et al., 2009), modifying hydrological cycle (Ramanathan and Carmichael, 2008), affecting food production and nutritional value (Lobell and Field, 2007; Jethva et al., 2019) and more recently in affecting human health (Cohen et al., 2017; Balakrishnan et al., 2019; Chowdhury et al., 2018). Exposure to air pollution has been conceived as the third most important causes of global deaths accounting approximately 7 million premature mortalities worldwide (WHO, 2018). In India, exposure to air pollution has been reported to be the second largest risk contributing disease burden after malnutrition (in 2016, Dandona et al., 2017). Approximately 1.24 million deaths in India are reported to be attributed by air pollution exposure (in 2017), 54% of which are particularly due to the exposure of ambient particulate matter (Balakrishnan et al., 2019). However, magnitude of such multi-lateral impacts depends on several factors; especially the size, morphology and composition of particulates which in most cases, are direct function of particulate sources and prevailing meteorology (Cao et al., 2012; Lelieveld et al., 2015). Therefore, to delineate an effective air quality management plan it is absolutely necessary to accurately identify particulate sources and to quantify their relative contribution to total particulate mass.

Among many global aerosol hotspots, the Indo-Gangetic Plain (IGP) in South Asia is unique in terms of having the highest aerosol loading (Kumar et al., 2018; Dey and Di Girolamo, 2011) and by the presence of diverse kind of particulates (Kedia et al., 2014; Gautam et al., 2011), with considerable spatial (Giles et al., 2011; Mhawish et al. 2017; Sen et al., 2017), temporal (Jethva et al., 2005; Kumar et al., 2018) and vertical variations (Vinjamuri et al., 2020; Mhawish et al., 2020). Despite being a region with high susceptibility to air pollution; information on sources of airborne particulates and their relative contributions are considerably limited over IGP, evident particularly over few urban agglomerates and often concluded with limited observations (Banerjee et al., 2015; Pant and Harrison, 2012). Likewise, sources of airborne particulates (both $PM_{2.5}$ and PM_{10}) across IGP are reported primarily from Karachi (Mansha et al., 2012), Delhi (Chowdhury et al., 2007; Shridhar et al., 2010; Sharma et al., 2014), Agra (Singh and Sharma, 2012), Kanpur (Chakarborty and Gupta, 2010; Behera et al., 2011), Kolkata (Chowdhury et al., 2007; Gupta et al., 2007, 2008) and Dhaka (Begum et al., 2007). In priority of the cases, fossil fuel combustion and biomass burning emissions were recognized as principal sources of fine particulates whereas, crustal resuspensions (and road dust) were reported as main source for coarse particulates. Similar conclusion was drawn by Singh et al. (2017) for $PM_{2.5}$ sources across South Asia; referring vehicular emissions, industrial pollution and secondary aerosols as the dominating sources. However, nature and contribution of particulate

sources varies considerably with respect to space and time, and often remain incomparable due to non-uniformity in marker selection, collinearity of varied sources, and/or due to methodological uncertainties (Banerjee et al., 2015; Pant and Harrison, 2012). Besides, inter-comparability of source apportionment studies also constrains by the fact that monitoring sites are often representative of a particular emission source or season. Source apportionment of airborne particulates are exceedingly rare (if not none) over rural and semi-urban locations across IGP and only in limited instances, long-term monitoring data was considered for identifying sources. Such knowledge gap severely limits the causal association of particulate sources and their health impacts thereby, confining effectiveness of air quality control measures.

For this submission, we focused only on central part of IGP as the region has limited number of air monitoring network (and data) with very limited reported instances of characterization of particulate sources. The central part of IGP also holds a unique characteristic of accumulating airborne particulates from the upper IGP by prevailing westerlies (Kumar et al., 2017; Sen et al., 2017). Besides, formation of anti-cyclonic zone facilitates subsidence of particulates from a greater height (Dey and Di Girolamo, 2011). Seasonal variations in localized particulate sources also influence physio-chemical and optical properties of aerosols (Mhawish et al., 2017; Gautam et al., 2011; Kedia et al., 2014). Contribution by different particulate sources and due to meteorological influences, a diverse and dynamic kind of particulate is generally evolved over central IGP which induce fundamental uncertainties in understanding aerosol-climate-health interactions over the region. This initiate the scope of this research to initially identify particulate sources over central IGP and to associate particulate-bound metals with human health. Two monitoring locations were therefore, categorically selected, one representing an urban habitat and the other more with a rural background. Further, non-carcinogenic health risks associated with airborne particulates were also investigated.

2. Experimental location and data analysis

2.1 Study area

Continuous monitoring of airborne PM_{10} was performed both in Varanasi ($25^{\circ} 18' N$, $83^{\circ} 01' E$, 82.2 m above sea level) and in Mirzapur ($82^{\circ} 35' E$, $25^{\circ} 02' N$, 89.1 m above sea level). Both locations represent a common geographical region i.e. central Gangetic plain, although Varanasi is more of an urban city with high population load with frequent influx of tourists, whereas Mirzapur is a rural area surrounded mainly by agricultural and barren land (Fig. 1). Varanasi itself devoid of any major industrial activities except having some small-scale industries like food processing, paint manufacturing, batteries and few manufacturing industries. However, the city also receives

pollutants primarily from the upper IGP by the prevailing westerly blowing across the plain (Kumar et al., 2017; Singh et al., 2018; Sen et al., 2017). Vehicular emissions, road dust and crustal resuspensions with biomass and refuse burning are considered to be the major sources of airborne particulates in Varanasi. In comparison, the monitoring location in Mirzapur represents a rural background, with limited vehicular and commercial activities. Wind induced crustal resuspension coupled with biomass burning for residential cooking and heating purposes are major emitters of air pollutants. Both the stations typically experience a humid sub-tropical climate; while Varanasi does not experience any localized effect of ocean or mountain, Mirzapur is surrounded by several small hills which may influence free dispersion of pollutants. Particulate movement is further constrained by the convective movement of air as the region experiences significant diurnal variation of atmospheric boundary layer (Murari et al., 2017).

2.2 Monitoring of airborne particulates

Particulate monitoring was carried out with respirable dust sampler (APM 460 BL; Envirotech). Both coarse (PM_{10}) and total-suspended particulate matter (TSPM) were monitored during the entire period, while particulate composition and sources were only characterized for PM_{10} fraction. Sampler was run once in a week continuously for 24 h for three years in Mirzapur (December 2014 – December 2017). In Varanasi, particulate sampler was run for 24 h for four years (January 2014 – December 2017); once/ twice a week during monsoon (JJAS) and post-monsoon (ON) while during summer (MAM) and winter (DJF), sampling was carried out often in each alternative days. Particulates have been deposited on preconditioned 8" X 10" glass fiber filter (Whatman). Filter papers were desiccated 24 h both before and after exposure, and deposition was measured by gravimetric method (AY220, Shimadzu) in humidity and temperature-controlled room. The exposed filters were further stored at -20°C till the completion of all the analysis.

2.3 Analysis of elemental and water-soluble inorganic ions

Exposed filter papers were digested using di-acids (5.55% HNO_3 and 16.67% of HCl) on a hotplate for 2 h following USEPA IO-3.2 method (EPA, 1999). Digested filters were filtered (No. 42, Whatman) and analysed for Ca, Fe, Mg, Na, Cu, Co, Cr, Mn, Pb, Cr, Cd, Zn, K, Ni by the atomic absorption spectrophotometer (Avanta Ver 2.01, GBC), having 10% of blank samples to make corrections. Standard recovery tests were made by spiking with a known amount of metal and following identical sample treatment procedure. The range of recovery efficiencies among the metals varied in between 93% (Cu) and 100% (Ni).

Water-soluble inorganic species (WSIS) were analyzed with the help of ion chromatograph (ICS-3000, Dionex, USA). Samples were initially ultrasonicated for 90 min with deionized water,

followed by filtration using a syringe filter (pore size 0.2 μm). Concentration of anions (F^- , Cl^- , NO_3^- and SO_4^{2-}) were measured using an anion micro-membrane suppressor (ASRS-300, 4 mm; Dionex, USA) with IonPac analytical column (AS11-HC X 250 mm). All the cations (NH_4^+ , K^+ , Ca^{2+} and Mg^{2+}) were analyzed using suppressor (CSRS-300, 4 mm; Dionex, USA) with a separation column (IonPac CS17-HC, 4 \times 250 mm; Dionex, USA) having a guard column (IonPac CG17-HC, 4 \times 50 mm; Dionex, USA). The detail procedure for extraction and WSIS analysis are mentioned in Murari et al. (2015) and in Singh et al. (2018).

2.4 Source apportionment of particulate

Principal component analysis (PCA) is a common form of factor analysis used often to reduce number of variables, and helps to transform data into few liner combinations without much loss of information (Banerjee et al., 2015; Ghosh et al., 2018). Here, PCA was run only as an exploratory tool to identify suitable set of principal components in the particulate speciation dataset. PCA was run on entire composition data measured individually in both the stations, without any data treatment and irrespective of any seasonal classification. To run both PCA and UNMIX, a similar set of data was used where negative or zero values were replaced with half of the method detection limit and missing values were replaced by arithmetic means of the closest observation. Besides, only those variables that justify its selection in UNMIX based on specific variance <0.5, were included in the PCA. To get suitable set of principal components, several options like change in number of the factors, Eigen value threshold, variance (%) and rotation of the principal component loadings were explored.

Identification of particulate sources and their respective contribution was made by confirmatory factor analysis using UNMIX (V6.0), an advanced receptor model developed by USEPA (epa.gov/air-research/unmix, accessed on January, 2019). The UNMIX is a multivariate receptor model that seeks edge points in data matrix to identify the particulate sources. These edge points are the spaces where enrichment of the specific chemical species is very low (or null, Henry, 2003). Through geometrically driven approach, UNMIX detect edges in the data matrix by singular value decomposition method (SVD, Banerjee et al., 2015). It assumes that during the monitoring period there are samples which contains very minimal or almost no enrichment from a specific source to differentiate the contribution. The model can be expressed as:

$$C_{ij} = \sum_{l=1}^p \left(\sum_{k=1}^p U_{ik} D_{kl} \right) V_{lj} + \varepsilon_{ij} \quad (1)$$

where U , D , and V are $n \times p$, $p \times p$ diagonal, and $p \times m$ matrices, respectively. ε_{ij} is the error consisting all the variability in C_{ij} not accounted by first principal components (p). Like other confirmatory factor

analysis, UNMIX does not require preidentified source profile which makes it readily applicable for diverse region. To run UNMIX, similar dataset was used as to run PCA; negative or zero values were replaced with half of the method detection limit, missing values were replaced by arithmetic means of the closest observation and species with >50 percent of the variance due to error (or specific variance, $SV > 0.5$) was considered for exclusion. The model has been used in several source apportionment studies both globally (Henry, 2000; Larsen and Baker, 2003; Maykut et al., 2003; Mukerjee et al., 2004) and in India (Chakraborty and Gupta, 2010; Tiwari et al., 2013), and has produced satisfactory results.

2.5 Particle backward trajectory

To understand the origin and trans-boundary movement of air mass over the sampling locations, NOAA HYSPLIT backward trajectory model (Hybrid Single Particle Lagrangian Integrated Trajectory; Draxler and Rolph, 2003) was run using archived meteorological dataset. Five-days (120 h) air mass back-trajectories were plotted at an altitude of 500 m (AMSL) using the Global Data Assimilation System data (GDAS, $0.5^\circ \times 0.5^\circ$) available at <http://ready.arl.noaa.gov/gdas1.php>. However, instead of plotting particle transport for each monitoring days; backward trajectories were only simulated for 20% of low PM_{10} loading days (Varanasi: $< 80 \mu g m^{-3}$, N: 86; Mirzapur: $< 75 \mu g m^{-3}$, N: 30) and 20% very high PM_{10} loading days (Varanasi: $> 250 \mu g m^{-3}$, N: 89; Mirzapur: $> 175 \mu g m^{-3}$, N: 34), to distinguish any specific movement of air mass that is influencing local particulate concentration. Besides, concentration weighted trajectories (CWT; Wang et al., 2009; Kumar et al., 2018) were also drawn on similar conditions, considering surface particulate concentration to recognize potential source fields and their relative contribution.

2.6 Geo-accumulation index

Geo-accumulation index (I_{geo}) helps to assess the extent of heavy metals contamination in airborne particulate by comparing their particulate-bound concentration against concentration found in the Earth crust. Here, it was used to provide an estimate for anthropogenic influence on trace metals and was computed based on equation (2) given by Muller (1979)

$$I_{geo} = \log_2 [C_{e(sample)} / 1.5 * C_{e(crustal)}] \quad (2)$$

where, $C_{e(sample)}$ and $C_{e(crustal)}$ is the concentration of species 'e' in sample and earth crust, respectively. The I_{geo} have seven classes defining pollution level from uncontaminated to extremely contaminated (Nowrouzi and Pourkhabbaz, 2014; Izhar et al., 2016).

2.7 Human health risk assessment

2.7.1 Exposure dose assessment

Health risk assessments of a species depend upon the pathways i.e. by ingestion (ing.), inhalation (inh.) and by dermal contact (der.), through which the specific species come into the contact of a human body. Human body exposures are computed for particulate-bound individual element in terms of average daily dose of exposure following USEPA (2009) guideline. Average daily exposure dose of PM₁₀-bound heavy metals (mgkg⁻¹day⁻¹) were calculated as:

i. Through ingestion (ADDE_{ing})

$$ADDE(ing) = CE \frac{IngR * Exp Freq * Exp Dur * Conv Fact}{Body Weight * Avg Time} \quad (3)$$

ii. Through inhalation (ADDE_{inh})

$$ADDE(inh) = CE \frac{InhR * Exp Freq * Exp Dur}{Body Weight * Avg Time * Part Emiss Fact} \quad (4)$$

iii. Through dermal contact (ADDE_{derm})

$$ADDE(der) = CE \frac{Skin Area * Adh Fac * Event Freq * ABS * Exp Freq * Exp Dur * Conv Fact}{Body Weight * Avg Time} \quad (5)$$

where, *ADDE* is the average daily intake of the particular element (μgkg⁻¹day⁻¹); *CE*, concentration of element in PM₁₀ (μgm⁻³); *IngR*, ingestion rate (children: 60; adults: 30 mg day⁻¹); *Exp Freq*, exposure frequency (365 yr⁻¹); *Exp Dur*, exposure duration (children: 6; adults: 24 years); *Conv Fact*, to convert mg kg⁻¹ to kg kg⁻¹; *Body Weight* (children: 15; adult: 70 kg); *Avg Time*, average time period in days which was calculated as *Exp dur* * 365; *InhR*, inhalation rate (children: 20; adult: 7.63 m³ day⁻¹); *Part Emiss Fact*, particle emission factor (1.36*10⁹ m³kg⁻¹); *Skin Area*, exposed skin surface area (children: 2800; adults: 5700 cm²); *Adh Fac*, adherence factor (children: 0.2; adults: 0.07 mg cm⁻²h⁻¹); *Event Freq*, event frequency (one event per day); *ABS*, dermal absorption factor (0.001 for both children and adult) (USEPA, 2007, 2009, 2011; Izhar et al., 2016).

2.7.2 Non-carcinogenic health risk

Non-carcinogenic health risk due to PM₁₀-bound heavy metals is measured in terms of Hazard quotient (HQ) and Hazard index (HI). HQ was calculated by dividing average daily dose of exposure with the reference daily intake (RfD). Since multiple elements are involved with PM₁₀, hence their collective effect (HI) was the integration of individual HQs (Zheng et al., 2010). HI values >1 indicate existence of significant non-carcinogenic health risk and <1 indicate no significant risk (US EPA, 2001).

$$HQ(ing/inh/der) = \frac{ADD(ing)/(inh)/(der)}{RfD(ing),(inh),(der)} \quad (6)$$

$$HI = \sum_{i=1}^n HQ_i \quad (7)$$

3. Results and discussion

3.1 Characteristics of particulate concentration

Ambient air quality both in terms of suspended respirable particulate (PM_{10}) and total-suspended particulate (TSPM) was measured in two contrasting locations over central IGP, and a total of 435 (Varanasi) and 169 (Mirzapur) particulate samples were analyzed for particulate mass (Fig. 2) and composition (Fig. 3-4). Overall mean PM_{10} concentration in Varanasi was $178 (\pm 105) \mu g m^{-3}$ (mean \pm SD), representing 65% of total particulate loading ($273 \pm 145 \mu g m^{-3}$). The annual mean concentration was comparable to the reported concentration of $176 (\pm 85) \mu g m^{-3}$ by Murari et al. (2015) for year 2013. In Mirzapur, the annual average loading of PM_{10} and TSPM was $131 (\pm 56) \mu g m^{-3}$ and $195 (\pm 71) \mu g m^{-3}$, respectively. Both the stations revealed a very high particulate concentration well above the standard as prescribed by Central Pollution Control Board ($60 \mu g m^{-3}$) and WHO ($20 \mu g m^{-3}$). Average ratio of PM_{10} to TSPM varied in between 0.64 and 0.66, signifying considerable proportion of total particulate loading was consist of particulates with aerodynamic diameter less than $10 \mu m$.

We also note a marked seasonality in particulate concentration with post-monsoon and winter months are in general having very poor air quality with 100% exceedance in PM_{10} concentration compared to national standard. This is in comparison to 62% (Mirzapur) and 72% (Varanasi) of exceedance on an annual basis. During winter season, average PM_{10} concentration in Varanasi was $268 (\pm 105) \mu g m^{-3}$ with a 24 h maximum of $535 \mu g m^{-3}$. Indiscriminate burning of biomass especially for household cooking and residential heating, waste incineration, vehicular emissions, dusts/ soils are often considered as the prime sources of PM_{10} at Varanasi. Except winter, relative concentration of PM_{10} was comparable during summer ($176 \pm 73 \mu g m^{-3}$) and post monsoon ($167 \pm 70 \mu g m^{-3}$). In contrast, there was no such difference in between winter ($168 \pm 49 \mu g m^{-3}$) and post-monsoon seasons ($172 \pm 65 \mu g m^{-3}$) in Mirzapur with lowest concentration noted during monsoon season ($68 \pm 20 \mu g m^{-3}$).

3.2. Composition of particulates

Composition of airborne particulate and their relative variations are shown in figure 3 and descriptive statistics are included in Table S1-S2 (supplementary file). Among the identified elements, Ca and Fe contributed the most both in Varanasi and Mirzapur. Overall, elemental species

contribute 15% of PM_{10} concentrations in Varanasi with primary contribution from Ca (9.1%) and Fe (1.9%; Fig. 4). Among the other elements, Na (1.0%), K (1.0%) and Zn (1.3%) were also found to enrich particulate mass. The contribution of elemental species did not vary considerably among the seasons (summer: 16.5%; winter: 16.7%), and both Ca (10%) and Fe (2%) contributed the major fraction of particulate mass during both the seasons. The monitoring location in Mirzapur represents a rural background, thereby dominance of crustal originated species was expected. On annual basis, elemental species contributed 18% of particulate mass in Mirzapur, that too primarily influenced by Ca (7.2%) and Fe (3.0%). Minor contributions from Zn (2.6%), K (1.8%) and Na (1.6%) were also noted. Within the detectable limit of metallic concentrations, Ca, Fe, Mg and Na were prevalent both in Mirzapur and in Varanasi, signifying primary contribution of crustal resuspensions while presence of other elements like Fe and K indicate contribution from biomass and waste burning. Presence of PM_{10} bound trace amount of Zn (1.3%-2.7%), particularly during winter months (3.7%-5.5%) may be an indication of emissions from burning of residual oil, refuse and garbage (Gonzalez et al., 2016).

Among the WSIS; SO_4^{2-} , NO_3^- , NH_4^+ constitute the major fraction of PM_{10} mass followed by traces of K^+ , Cl^- and F^- . In Varanasi, annually averaged WSIS accounted approximately 19% of particulate mass, that too varied considerably among the seasons (summer: 16.0%; winter: 21.3%). Major ions contributed to PM_{10} mass was SO_4^{2-} (6.7%), NO_3^- (3.9%) and NH_4^+ (2.8%) followed by Cl^- (3.0%). The secondary inorganic species ($SIA = SO_4^{2-} + NO_3^- + NH_4^+$) accounted 13.4% of the particulate mass concentration, comparatively high during winter (15.7%) against summer months (12.1%). Similar was the case in Mirzapur, where SIA contributed almost 11.9% of particulate, with significant variation between summer (10.8%) and winter months (18.7%). The variation in ionic contribution among the seasons was mainly influenced by SO_4^{2-} (summer: 4.7%; winter: 8.6%), NO_3^- (summer: 4.0%; winter: 5.6%) and NH_4^+ (summer: 2.1%; winter: 4.7%). For both the stations, SIA contribute the major fraction of particulate mass during winter months indicating secondary nature of PM_{10} sources over the region (Saxena et al., 2017, Murari et al., 2015). It is worth to mention that particulate-bound water-soluble Ca^{2+} and Mg^{2+} were also detected in high abundance (4-7% of PM_{10} mass) in both the locations but was not reported here, as both the species were rich in element form compared to its ionic form. We also tried to constitute the sources of particulate-bound nitrogen and sulfur using NO_3^- to SO_4^{2-} ratio as a proxy for mobile and stationary source contribution (Tian et al., 2016). The ratio of water-soluble NO_3^-/SO_4^{2-} for Varanasi was 0.75 (± 0.76) and 0.83 (± 0.18) for Mirzapur, both representing dominance of stationary sources. However, NO_3^-/SO_4^{2-} ratio reduced during the months of winter (Varanasi: 0.59; Mirzapur: 0.65) referring increase in stationary source contribution, particularly from the burning of fuels for residential heating. The contribution of biomass burning was also noted by the added contribution of K^+ and NH_4^+ ion during winter months.

Both K^+ and NH_4^+ ions are indicator of biomass burning emissions and their relative contribution to PM_{10} mass concentration increased during winter for both in Varanasi (K^+ : 2.0% NH_4^+ : 3.2%) and in Mirzapur (K^+ : 1.6% NH_4^+ : 4.7%). It is to be noted that organic fraction (representing both aliphatic and aromatic organics) associated with PM_{10} was also assessed by organic solvent extraction process following ASTM (2010). Solvent extracted organic fraction (OF) constitute 19%-23% of particulate mass. However, due to non-availability of organic speciation dataset, this was not included in the multivariate factor analysis.

3.3. Identification of major sources

We used Principal Component Analysis (PCA) initially to identify principal factors (or components) that explain the maximum variance within the particulate speciation dataset. PCA is a method for multivariate factor analysis which is often used as an exploratory tool to quantify source contribution by combining factor analysis with a multi-linear regression model (Viana et al., 2008; Ghosh et al., 2018). The factors identified by the PCA was used to share the entire variability of the datasets and factor with maximum variance was interpreted as the most influential source. We performed PCA on entire particulate composition dataset measured in both the stations, without any data treatment and irrespective of any seasons (Fig. S1). However, only those variables were included in the PCA that also justified its selection in UNMIX based on specific variance. Therefore, species like F^- and Cl^- were not included in the analyses as they induced higher uncertainty. A total of five factors were sorted having eigen value >1 . All the factors in combination explain $>92\%$ of variance for Varanasi (92.6%) and Mirzapur (96.06%). The principal factors identified by PCA are:

Factor 1. The first factor indicates a high dominance of Ca, Fe, Mg, Na and explain 52% to 56% of variance for Mirzapur and Varanasi, respectively. Both Ca, Fe and Mg are considered to be originated from Earth's crust which become airborne by prevailing wind (Banerjee et al., 2017), while Mg and Na also pose crustal signature as there was no intrusion of marine aerosols (Pant and Harrison, 2012).

Factor 2. This was mainly enriched by the species like Co, Cu, Cr, Pb contributing 15% to 17% of variance for both the stations. Both Pb and Cu are internationally accepted marker of vehicular emissions as Pb typically used as additive in Petrol, before being phased out from India in year 2000. Emission of Cu and traces of Cr are linked with brake linings emissions. In Factor 2, presence of Ni, Cd and Co in significant loading were also noted in Mirzapur. Presence of Ni is a possible indicator of combustion of heavy oil (Khare and Baruah, 2010) while Cd and Co is an established marker of industrial emissions. That possibly indicate that the factor 2 was a combination of vehicular emissions mixed with industrial sources.

Factor 3. Enriched with the elemental species like K, Zn, Mn with K^+ with a contribution of 13-16% of variance. The K^+ is an established marker of biomass/ wood combustion where there is no influence of marine aerosols (Singh et al., 2018). Particulate bound Zn mainly emits from burning of residual oil, refuse, and garbage with greater accumulation in coarser particulates (Gonzalez et al., 2016). So, this factor indicates emission from biomass burning with added contribution from waste/ refuse incineration. However, a moderate loading of Mn and Ca indicate that occasionally the factor may also be influenced by various other emission sources (like crustal/road dust, industrial emissions).

Factor 4. This factor shows loading of secondary inorganic aerosols (SO_4^{2-} , NO_3^- and NH_4^+) which are well accepted marker for secondary aerosols originated mainly from photochemical reactions of primary species. Individually, agricultural and industrial emissions are linked with NH_4^+ emission while SO_4^{2-} is attributed to coal combustion and wood burning. Primary emissions of NO_x and SO_2 however, gradually transform by photochemical reactions and constitute various salts via gas-to-particle conversion. For both the stations, secondary aerosols were found to share 9%-10% of variance.

3.4 Particulate sources identified by UNMIX

Possible sources of airborne particulate in Varanasi and Mirzapur was quantified by confirmatory factor analysis using UNMIX (V6.0). Initially, UNMIX was applied in entire particulate dataset (Varanasi: 435; Mirzapur: 169) with all the measured elemental and WSIS species excluding F^- and Cl^- (due to higher variability, specific variance >0.5). Besides, dataset was also classified for two prominent seasons i.e. summer (Varanasi: 149; Mirzapur: 53) and winter (Varanasi: 125; Mirzapur: 50), to identify the seasonal variations of prominent sources. Identical source signature was considered that was also used in multivariate factor analysis like PCA. The source apportionment of particulate measured during monsoon and post-monsoon was not achieved due to limited dataset therefore, was only included in the annual data profile.

Overall, UNMIX was able to extract particulate sources for both the locations with crustal resuspensions (dust/-soil) sharing the prominent proportion of particulate sources throughout the monitoring period (Fig. 5). Dust and crustal elements suspended by wind contribute almost 63% of PM_{10} sources in Varanasi, which typically enhanced during summer months (71%) compared to winter (51%). The most prominent source for PM_{10} in Mirzapur was also crustal resuspensions, contributing 57% of total PM_{10} mass, while being slightly higher during winter (70%) compared to summer months (61%). During summer, the crustal elements were found to be mixed with Cu and Pb in Mirzapur, indicating added contribution from vehicular emissions and road dusts. Characteristically, both summer and winter months are dry across IGP with minimum rainfall (Murari

et al., 2017) which induce a greater resuspension of airborne particulate into the atmosphere. Besides, being mainly a land-locked region, the advective movement of pollutants over central IGP are rather low compared to convective movement which induce large-scale lifting of aerosols to a greater height, particularly during summer months (Gautam et al., 2011). Therefore, resuspension of dust/ soil through prevailing wind contribute a considerable proportion of coarse particulates over the region, which may only be controlled by increasing green cover, both by promoting urban forestry and creating artificial forest cover.

The second important source of PM_{10} that emerge out is secondary aerosols, which are the photochemical products (ammonium sulphate and ammonium nitrate, secondary organics etc.) of primary precursors (VOCs, NH_3 , SO_2 and NO_x), which transforms to condense phase both by gaseous and liquid-phase reactions. Ideally, the contribution of secondary aerosols and aerosols (and its precursors) emitted from biomass burning emissions have common source signature and therefore, in most cases discriminating their individual contribution to total particulate loading is critical. Here, secondary aerosols were found to contribute 17% of PM_{10} mass in Varanasi that varied within a range of 14% (summer) to 37% (winter). Similar was the case for Mirzapur, where secondary aerosol contributed 23% of particulate mass. However, during summer, secondary aerosols were also mixed with traces of Cd and Ni, indicating added contribution from industrial sources.

The contribution of biomass (and waste/-refuse) burning emissions to PM_{10} loading was also assessed. The higher contribution of biomass burning emissions in Mirzapur (19%; 7%-25%) compared to Varanasi (10%; 4%-9%) was essentially due to the massive use of biomass-based fuels both for residential cooking and heating purposes (Banerjee et al., 2017). Besides, Mirzapur is the hub of many brick kilns which are particularly active during summer months and use of biomass-based fuels like cow dung cake, fuel residues, coal, wood are very common. Inefficient combustion within these furnaces potentially emits huge quantities of particulate matter (Begum et al., 2007). This possibly the reason behind increase contribution of biomass and refuse burning emissions in Mirzapur during summer months. The contribution of vehicular emissions in PM_{10} mass concentration for both the stations was within a range of 2%-9%. Vehicular emissions primarily contribute fine particulate of size $<2.5 \mu m$ therefore, their relative contribution to PM_{10} was expected to be less. Here, vehicular emissions were traced by the presence of Cu and Pb. However, presence of Co, Cd and Ni particularly during winter months in Mirzapur possibly indicate that vehicular sources were also mixed with industrial sources.

The nature of PM_{10} sources over central IGP was comparable to that of reported sources for other cities across IGP like Delhi (Srivastava and Jain, 2007; Srivastava et al., 2009; Khillare and Sarkar, 2012); Kanpur (Shukla and Sharma, 2008); Agra (Singh and Sharma, 2012) and in Dhaka

(Begum et al., 2007). All these studies concluded the major contribution of crustal resuspensions as the prime source of PM_{10} . However, there are instances when contribution of secondary sources (Delhi, Sharma et al., 2014) and waste disposal (Kolkata, Karar and Gupta, 2007) were also held responsible for PM_{10} emissions.

3.5 Potential particulate source filed and transport

To understand possible origin of airborne particulates and transport through prevailing air mass, 5-days back-trajectories were plotted over both the sites at 500m AMSL (Fig. 6a-d). For both the stations, during low particulate loading days (Varanasi: $<80 \mu g m^{-3}$; Mirzapur: $<75 \mu g m^{-3}$), both marine and continental air masses contributed to particulate loading. Primary origin of marine air masses were Arabian Sea and Bay of Bengal whereas, continental air masses were mainly from western semi-arid region, Central highlands and Deccan Plateau; with very few originated from upper IGP. This was in contrast to high particulate loading days (Varanasi: $>250 \mu g m^{-3}$; Mirzapur: $>175 \mu g m^{-3}$) when almost all the air masses have originated from upper IGP e.g. northern parts of Pakistan, Punjab (India) and western semi-arid region. The CWT (Fig. 6e-f) also reciprocates the particulate transport pathways identifying the upper IGP as the most important source region, both during high and low particulate loading days. This certainly establish the westerlies as prominent wind to facilitate transport of pollutants from upper IGP to central IGP, which has also been reported by other contemporary researchers; especially during pre- (Sen et al., 2017) and post-monsoon (Singh et al., 2018) and in winter season (Kumar et al., 2017).

3.6 Assessment of PM_{10} bound metal contamination

Particulate-bound metal contamination was evaluated in terms of Geo-accumulation index (I_{geo}). The I_{geo} for PM_{10} bound metals in Varanasi and Mirzapur with classes for degree of contamination are shown in Figure 7. Intra-species contamination for all the metals varied considerably and except Co, I_{geo} remain comparable for both the locations. The degree of contamination by Cd was none ($I_{geo} < 0$) whereas in Mirzapur, exposure to Cu, Pb and Ni showed moderate contamination (I_{geo} : 1-2). The same remain true for Varanasi as exposure to PM_{10} bound Pb indicate moderate contamination in contrast to Co, Cu and Cr, which showed moderate to strong contamination (I_{geo} : 2-4). Overall, for both the sites the highest level of contamination appears due to the presence of Ca, Mg, Na, K and Fe ($I_{geo} > 10$) followed by Mn and Zn (I_{geo} : 6-8). Strong enrichment of the elements like Ca, Mg, Na, K, Fe, Mn and moderate enrichment of Co, Cu, Cr and Zn indicate that over central IGP, particulate sources like crustal resuspensions, vehicular and biomass/ refuse burning do instigate considerable level of threat to human beings.

3.7 Human health risk assessment

The average daily dose of exposure (ADDE) was used to assess the non-carcinogenic threat of PM₁₀ bound heavy metals through different exposure pathways *viz.* ingestion, inhalation and dermal contact. The ADDE both for adults and children for individual metals are included in Table S3 (supplementary file). It indicates that, health risk induced by PM₁₀ bound metals are much higher in children compared to adults, possibly because of higher rate of exposure (like IngR, InhR) for children and due to lower body weight. Both in Varanasi and Mirzapur, exposure risk is lowest by inhalation and highest for ingestion in both the age groups. Almost in all the cases, exposure risks are higher in an order of 1 to 3 by ingestion, also reported in other case studies, like in Kanpur (Izhar et al., 2016) and in West Bengal (Ghosh et al., 2018).

Non-carcinogenic health effects of PM₁₀ bound metals are also assessed in terms of hazard quotient (HQ) and hazard index (HI), and are shown in Figure 8 (Table S4). Children were found to experience high non-carcinogenic health effects compared to adults. For individual metals, the HQ was measured high in Varanasi compared to Mirzapur, because of high contamination levels in urban environment compared to rural areas. Exposure to Cr, Pb (in Varanasi) and Cd (in Mirzapur) through ingestion shows highest hazardous effect in both age groups. In both the sites, low HQ values (<1) signify non-carcinogenic health risk is within the permissible limit. However, high HI values of carcinogenic elements (like Cr and Cd) compared to other heavy metals signify that in future, HI may exceed if adequate policies are not implemented to control emissions of particulate matter.

Conclusions

Considering the limited observation of particulate sources across IGP, present study was conducted to apportion the sources of airborne particulate, their relative contribution and seasonal variations. Besides, health risk posed by particulate bound metals to various age groups was also evaluated. Two contrasting locations were selected, one representing a rural and other as an urban background. Average concentration of PM₁₀ in between 2014 and 2017 was 178 (±105) µgm⁻³ (Varanasi) and 131 (±56) µgm⁻³ (Mirzapur). Twenty-four hours average PM₁₀ concentration frequently exceeded the air quality standard throughout the year, with maximum exceedance particularly in winter. The ratio of PM₁₀ to total particulate loading (0.64-0.66) signify the abundance of coarser fraction in ambient environment of Varanasi and Mirzapur. Overall, elemental species constitute 15% (Varanasi) and 18% (Mirzapur) of PM₁₀ concentration, with prevalence of Ca, Fe, Mg and Na. The WSIS accounted 15%-19% PM₁₀ mass, with primary contribution from SIA (SO₄²⁻, NO₃⁻, NH₄⁺), followed by Cl⁻ with considerable seasonal variations that were associated to the changes in emission types. The average ratio of NO₃⁻/SO₄²⁻ for Varanasi and Mirzapur were less than unity,

representing the dominance of stationary sources. Initially, PCA was run to identify principal factors in particulate speciation dataset and to access their possible origin. Five factors were sorted having eigen value >1 and explaining total variance >92% for Varanasi and Mirzapur. The source contribution achieved by UNMIX on overall dataset indicate crustal resuspension (dust/-soil; Varanasi: 63%; Mirzapur: 57%) as the primary source of PM₁₀ concentration, followed by secondary aerosols, biomass and refuse burning and vehicular emissions. Contribution of particulates transported from upper IGP and north-western dry land to central IGP by prevailing westerlies were found to elevate regional pollution load. Hazard quotient of individual metals show higher contamination in Varanasi compared to Mirzapur. Non-carcinogenic health risk assessment confirms heavy metals associated health risk is within the permissible limit, although have potential to elevate if proper control measures are not adopted.

Acknowledgements

This research is financially supported by Science and Engineering Research Board, Department of Science and Technology, New Delhi (SR/FTP/ES-52/2014). TB acknowledges fund received from ASEAN- India S&T Development Fund, Govt. of India (CRD/2018/000011) under ASEAN- India Collaborative Research and Development Scheme. This research work is a part of doctoral thesis submitted by VM in IESD, BHU. Cooperation extended by Dr. Rajni Srivastava for particulate monitoring in RGSC, Mirzapur is also acknowledged. Authors are also thankful to the two anonymous reviewers for their valuable suggestions.

Author Contributions

VM and TB designed the research; VM, TB, NS, RR experimented, analyzed and interpreted the result. NS, TB and RSS drafted the manuscript.

Competing interests. Authors declare that they have no conflict of interest.

Reference

1. ASTM (2010). ASTM D4600-87 standard test method for the determination of benzene-soluble particulate matter in workplace atmospheres. American Society for Testing and Materials, USA
2. Balakrishnan, K., Dey, S., Gupta, T., Dhaliwal, R.S., Brauer, M., Cohen, A.J., Stanaway, J.D., Beig, G., Joshi, T.K., Aggarwal, A.N. and Sabde, Y., 2019. The impact of air pollution on deaths, disease burden, and life expectancy across the states of India: the Global Burden of Disease Study 2017. *The Lancet Planetary Health*, 3, e26-e39.
3. Banerjee, T., M. Kumar, R. K. Mall, and R. S. Singh. Airing 'clean air' in clean India mission. *Environmental Science and Pollution Research* 24, no. 7 (2017): 6399-6413.
4. Banerjee, T., Murari, V., Kumar, M., & Raju, M. P. (2015). Source apportionment of airborne particulates through receptor modeling: Indian scenario. *Atmospheric Research*, 164, 167-187.
5. Begum, B. A., Biswas, S. K., & Hopke, P. K. (2007). Source apportionment of air particulate matter by chemical mass balance (CMB) and comparison with positive matrix factorization (PMF) model. *Aerosol and Air Quality Research*, 7(4), 446-468.

6. Behera, S.N., Sharma, M., Dikshit, O., Shukla, S.P., 2011. GIS-based emission inventory, dispersion modeling, and assessment for source contributions of particulate matter in an urban environment. *Water Air Soil Pollut.* 218, 423–436.
7. Cao, J., Xu, H., Xu, Q., Chen, B., Kan, H., 2012. Fine particulate matter constituents and cardiopulmonary mortality in a heavily polluted Chinese city. *Environ. Health Perspect.* 120(3), 373–378.
8. Chakraborty, A., Gupta, T., 2010. Chemical characterization and source apportionment of submicron (PM₁) aerosol in Kanpur Region India. *Aerosol Air Qual. Res.* 10, 433–445.
9. Chowdhury, S., Dey, S. and Smith, K.R., 2018. Ambient PM 2.5 exposure and expected premature mortality to 2100 in India under climate change scenarios. *Nat. Commun.* 9(1), 318.
10. Chowdhury, Z., Zheng, M., Schauer, J. J., Sheesley, R. J., Salmon, L. G., Cass, G. R., & Russell, A. G. (2007). Speciation of ambient fine organic carbon particles and source apportionment of PM_{2.5} in Indian cities. *Journal of Geophysical Research: Atmospheres*, 112(D15).
11. Cohen AJ, Brauer M, Burnett R, et al. Estimates and 25-year trends of the global burden of disease attributable to ambient air pollution: an analysis of data from the Global Burden of Diseases Study 2015. *Lancet* 2017; 389: 1907–18.
12. Draxler, R.R., and Rolph, G.D., 2003. HYSPLIT (HYbrid single-particle Lagrangian integrated trajectory) model access via NOAA ARL READY. NOAA Air Resources Laboratory, Silver Spring, MD. <http://ready.arl.noaa.gov/HYSPLIT.php>.
13. Dandona, L., Dandona, R., Kumar, G. A., Shukla, D. K., Paul, V. K., Balakrishnan, K et al. (2017). Nations within a nation: variations in epidemiological transition across the states of India, 1990–2016 in the Global Burden of Disease Study. *The Lancet*, 390(10111), 2437–2460.
14. Dey, S., & Di Girolamo, L. (2011). A decade of change in aerosol properties over the Indian subcontinent. *Geophysical Research Letters*, 38(14).
15. EPA, (1999). National air quality and emissions trends report. Office of Air Quality Planning and Standards.
16. Gautam, R., Hsu, N. C., Tsay, S. C., Lau, K. M., Holben, B., Bell, S., ... and Payra, S. (2011). Accumulation of aerosols over the Indo-Gangetic plains and southern slopes of the Himalayas: distribution, properties and radiative effects during the 2009 pre-monsoon season. *Atmospheric Chemistry and Physics*, 11(24), 12841–12863.
17. Ghosh, S, Rumi Rabha, Mallika Chowdhury, and Pratap Kumar Padhy. Source and chemical species characterization of PM₁₀ and human health risk assessment of semi-urban, urban and industrial areas of West Bengal, India. *Chemosphere* 207 (2018): 626–636.
18. Giles, D. M., Holben, B. N., Tripathi, S. N., Eck, T. F., Newcomb, W. W., Slutsker, I., .. & Singh, R. P. (2011). Aerosol properties over the Indo-Gangetic Plain: A mesoscale perspective from the TIGERZ experiment. *Journal of Geophysical Research: Atmospheres*, 116(D18).
19. González, J. M., Torres-Mora, M. A., Keesstra, S., Brevik, E. C., & Jiménez-Ballesta, R. (2016). Heavy metal accumulation related to population density in road dust samples taken from urban sites under different land uses. *Science of the Total Environment*, 553, 636–642.
20. Gupta, A.K., Karar, K., Ayoob, S., John, K., 2008. Spatio-temporal characteristics of gaseous and particulate pollutants in an urban region of Kolkata, India. *Atmos. Res.* 87, 103–115.
21. Gupta, A.K., Karar, K., Srivastava, A., 2007. Chemical mass balance source apportionment of PM₁₀ and TSP in residential and industrial sites of an urban region of Kolkata India. *J. Hazard. Mater.* 142, 279–287.
22. Henry, R. C. (2000). UNMIX Version 2 Manual. Prepared for the US Environmental Protection Agency.
23. Henry, R. C. (2003). Multivariate receptor modeling by N-dimensional edge detection. *Chemometrics and intelligent laboratory systems*, 65(2), 179–189.
24. Izhar, S., Goel, A., Chakraborty, A., & Gupta, T. (2016). Annual trends in occurrence of submicron particles in ambient air and health risk posed by particle bound metals. *Chemosphere*, 146, 582–590.
25. Jethva, H., Satheesh, S. K., & Srinivasan, J. (2005). Seasonal variability of aerosols over the Indo-Gangetic basin. *Journal of Geophysical Research: Atmospheres*, 110(D21).
26. Jethva, H.; Torres, O.; Field, R. D.; Lyapustin, A.; Gautam, R.; Kayetha, V. (2019). Connecting Crop Productivity, Residue Fires, and Air Quality over Northern India. *Sci. Rep.* 2019, 9, 16594.
27. Karar, K., & Gupta, A. K. (2007). Source apportionment of PM₁₀ at residential and industrial sites of an urban region of Kolkata, India. *Atmospheric Research*, 84(1), 30–41.
28. Kedia, S., Ramachandran, S., Holben, B. N., & Tripathi, S. N. (2014). Quantification of aerosol type, and sources of aerosols over the Indo-Gangetic Plain. *Atmospheric environment*, 98, 607–619.
29. Khare, P., Baruah, B.P., 2010. Elemental characterization and source identification of PM_{2.5} using multivariate analysis at the suburban site of North-East India. *Atmos. Res.* 98 148:162.

30. Khillare, P. S., & Sarkar, S. (2012). Airborne inhalable metals in residential areas of Delhi, India: distribution, source apportionment and health risks. *Atmospheric pollution research*, 3(1), 46-54.
31. Kumar, M., Parmar, K. S., Kumar, D. B., Mhawish, A., Broday, D. M., Mall, R. K., & Banerjee, T. (2018). Long-term aerosol climatology over Indo-Gangetic Plain: Trend, prediction and potential source fields. *Atmospheric environment*, 180, 37-50.
32. Kumar, M., Raju, M. P., Singh, R. K., Singh, A. K., Singh, R. S., & Banerjee, T. (2017). Wintertime characteristics of aerosols over middle Indo-Gangetic Plain: Vertical profile, transport and radiative forcing. *Atmospheric Research*, 183, 268-282.
33. Larsen, R. K., & Baker, J. E. (2003). Source apportionment of polycyclic aromatic hydrocarbons in the urban atmosphere: a comparison of three methods. *Environmental science & technology*, 37(9), 1873-1881.
34. Lelieveld, J., Evans, J. S., Fnais, M., Giannadaki, D., & Pozzer, A. (2015). The contribution of outdoor air pollution sources to premature mortality on a global scale. *Nature*, 525(7569), 367-371.
35. Lobell, D. B., & Field, C. B. (2007). Global scale climate-crop yield relationships and the impacts of recent warming. *Environmental research letters*, 2(1), 014002.
36. Mansha, M., Ghauri, B., Rahman, S., & Amman, A. (2012). Characterization and source apportionment of ambient air particulate matter (PM_{2.5}) in Karachi. *Science of the total environment*, 425, 176-183.
37. Maykut, N. N., Lewtas, J., Kim, E., & Larson, T. V. (2003). Source apportionment of PM_{2.5} at an urban IMPROVE site in Seattle, Washington. *Environmental science & technology*, 37(22), 5135-5142.
38. Mhawish, A., Banerjee, T., Broday, D. M., Misra, A., & Tripathi, S. N. (2017). Evaluation of MODIS Collection 6 aerosol retrieval algorithms over Indo-Gangetic Plain: Implications of aerosols types and mass loading. *Remote Sensing of Environment*, 201, 297-313.
39. Mhawish, Alaa, K. S. Vinjamuri, Nandita Singh, Manish Kumar, and Tirthankar Banerjee. (2020). Vertical Profiling of Aerosol and Aerosol Types Using Space-Borne Lidar." In *Measurement, Analysis and Remediation of Environmental Pollutants*, pp. 165-177. Springer, Singapore.
40. Mukerjee, S., Norris, G. A., Smith, L. A., Noble, C. A., Neas, L. M., Özkaynak, A. H., & Gonzales, M. (2004). Receptor model comparisons and wind direction analyses of volatile organic compounds and submicrometer particles in an arid, binational, urban air shed. *Environmental science & technology*, 38(8), 2317-2327.
41. Müller, G., 1979. Schwermetalle in den Sedimenten des Rheins-Veränderungen seit 1971.
42. Murari, V., Kumar, M., Barman, S. C., & Banerjee, T. (2015). Temporal variability of MODIS aerosol optical depth and chemical characterization of airborne particulates in Varanasi, India. *Environmental Science and Pollution Research*, 22(2), 1329-1343.
43. Murari, V., Kumar, M., Mhawish, A., Barman, S. C., & Banerjee, T. (2017). Airborne particulate in Varanasi over middle Indo-Gangetic Plain: variation in particulate types and meteorological influences. *Environmental monitoring and assessment*, 189(4), 157.
44. Nowrouzi, M., & Pourkhabbaz, A. (2014). Application of geoaccumulation index and enrichment factor for assessing metal contamination in the sediments of Hara Biosphere Reserve, Iran. *Chemical Speciation & Bioavailability*, 26(2), 99-105.
45. Pant, P., & Harrison, R. M. (2012). Critical review of receptor modelling for particulate matter: a case study of India. *Atmospheric Environment*, 49, 1-12.
46. Ramanathan, V., & Carmichael, G. (2008). Global and regional climate changes due to black carbon. *Nature geoscience*, 1(4), 221-227.
47. Satheesh, S. K., Vinoj, V., Babu, S. S., Moorthy, K. K., & Nair, V. S. (2009). Vertical distribution of aerosols over the east coast of India inferred from airborne LIDAR measurements. In *Annales geophysicae: atmospheres, hydrospheres and space sciences* (Vol. 27, No. 11, p. 4157).
48. Saxena, M., Sharma, A., Sen, A., Saxena, P., Mandal, T. K., Sharma, S. K., & Sharma, C. (2017). Water soluble inorganic species of PM₁₀ and PM_{2.5} at an urban site of Delhi, India: seasonal variability and sources. *Atmospheric Research*, 184, 112-125.
49. Sen, A., Abdelmaksoud, A. S., Ahammed, Y. N., Banerjee, T., Bhat, M. A., Chatterjee, A. et al. (2017). Variations in particulate matter over Indo-Gangetic Plains and Indo-Himalayan Range during four field campaigns in winter monsoon and summer monsoon: role of pollution pathways. *Atmospheric environment*, 154, 200-224.
50. Sharma, S. K., Mandal, T. K., Saxena, M., Sharma, A., and Gautam, R. (2014). Source apportionment of PM₁₀ by using positive matrix factorization at an urban site of Delhi, India. *Urban climate*, 10, 656-670.
51. Shridhar, V., Khillare, P.S., Agarwal, T., Ray, S., 2010. Metallic species in ambient particulate matter at rural and urban location of Delhi. *J. Hazard. Mater.* 175, 600-607.

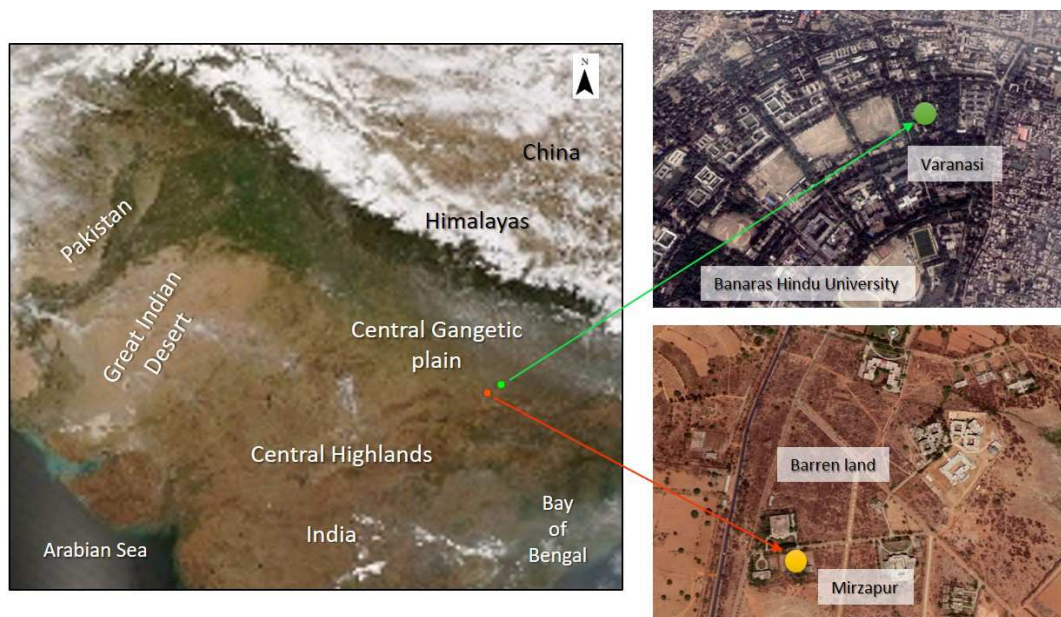
52. Shukla, S.P., and Sharma, M. (2008). Source apportionment of atmospheric PM₁₀ in Kanpur, India. *Environmental Engineering Science*, 25(6), 849-862.
53. Singh, N., Banerjee, T., Raju, M. P., Deboudt, K., Sorek-Hamer, M., Singh, R. S., & Mall, R. K. (2018). Aerosol chemistry, transport, and climatic implications during extreme biomass burning emissions over the Indo-Gangetic Plain. *Atmospheric Chemistry and Physics*, 18(19), 14197-14215.
54. Singh, N., Murari, V., Kumar, M., Barman, S. C., & Banerjee, T. (2017). Fine particulates over South Asia: Review and meta-analysis of PM_{2.5} source apportionment through receptor model. *Environmental Pollution*, 223, 121-136.
55. Singh, R., and Sharma, B. S. (2012). Composition, seasonal variation, and sources of PM₁₀ from world heritage site Taj Mahal, Agra. *Environmental monitoring and assessment*, 184(10), 5945-5956.
56. Srivastava, A., & Jain, V. K. (2007). Size distribution and source identification of suspended particulate matters in atmospheric aerosols over Delhi. *Chemosphere*, 68, 579-589.
57. Srivastava, A., Gupta, S., & Jain, V. K. (2009). Winter-time size distribution and source apportionment of total suspended particulate matter and associated metals in Delhi. *Atmospheric Research*, 92(1), 88-99.
58. Tian, M., Wang, H., Chen, Y., Yang, F., Zhang, X., Zou, Q., ... & He, K. (2016). Characteristics of aerosol pollution during heavy haze events in Suzhou, China. *Atmospheric Chemistry & Physics*, 16(11).
59. Tiwari, S., Pervez, S., Cinzia, P., Bisht, D.S., Srivastava, A.K., Chate, D., 2013. Chemical characterization of atmospheric particulate matter in Delhi, India, part II: source apportionment studies using PMF 3.0. *Sustain. Environ. Res.* 23 (5), 295–306.
60. U.S. EPA (U.S. Environmental Protection Agency), 2007. Guidance for Evaluating the Oral Bioavailability of Metals in Soils for Use in Human Health Risk Assessment.
61. U.S. EPA (U.S. Environmental Protection Agency), 2009. Risk Assessment Guidance for Superfund Volume I: Human Health Evaluation Manual (Part F, Supplemental Guidance for Inhalation Risk Assessment). Office of Superfund Remediation and Technology Innovation, Washington, D.C.
62. US EPA, 2001. Risk Assessment Guidance for Superfund: Volume III d Part a, Process for Conducting Probabilistic Risk Assessment. EPA 540-R-02 - 002. US Environmental Protection Agency, Washington, D.C.
63. US EPA, 2011. Risk Assessment Guidance for Superfund. In: Part, A. (Ed.), Human Health Evaluation Manual; Part E, Supplemental Guidance for Dermal Risk Assessment; Part F, Supplemental Guidance for Inhalation Risk Assessment, I.
64. WHO, 2018. <https://www.who.int/news-room/detail/02-05-2018-9-out-of-10-people-worldwide-breathe-polluted-air-but-more-countries-are-taking-action>. Accessed on February 29, 2020.
65. Wang, Y. Q., Zhang, X. Y., and Draxler, R. R.: 2009. TrajStat: GISbased software that uses various trajectory statistical analysis methods to identify potential sources from long-term air pollution measurement data, *Environ. Modell. Softw.*, 24, 938–939.
66. Viana, M., Kuhlbusch, T. A. J., Querol, X., Alastuey, A., Harrison, R. M., Hopke, P. K., Hitenberger, R. (2008). Source apportionment of particulate matter in Europe: a review of methods and results. *J Aerosol Sci.*, 39: 827-849.
67. Vinjamuri, K. S., Mhawish, A., Banerjee, T., Sorek-Hamer, M., Broday, D. M., Mall, R. K., & Latif, M. T. (2020). Vertical distribution of smoke aerosols over upper Indo-Gangetic Plain. *Environmental Pollution*, 257, 113377.
68. Zheng, N., Liu, J., Wang, Q., Liang, Z., 2010. Health risk assessment of heavy metal exposure to street dust in the zinc smelting district, Northeast of China. *Sci. Total Environ.* 408 (4), 726-733.

1 List of figures

- 2 Figure 1. Airborne particulate monitoring locations over central Indo-Gangetic Plain.
- 3 Figure 2. Monthly mean variations of airborne PM₁₀ and total particulate mass concentrations.
- 4 Figure 3. Distribution of particulate-bound elements and water-soluble ion concentrations.
- 5 Figure 4. Relative composition of particulate in (a) Varanasi and (b) Mirzapur.
- 6 Figure 5. Relative contribution of various sources to airborne particulates.
- 7 Figure 6. Potential particulate transport pathways (a-d) and source fields (e-h) during low and high PM₁₀
- 8 loading conditions in Varanasi (a,b,e,f) and Mirzapur (c,d,g,h).
- 9 Figure. 7. Geo-accumulation index of PM₁₀ bound metals and associated level of contamination.
- 10 Figure 8. Hazard Quotient (HQ) and Hazard Index (HI) for adults and children with respect to PM₁₀ bound
- 11 metal exposure.

12
13
14
15

16



17

18

Figure 1. Airborne particulate monitoring locations over central Indo-Gangetic Plain .

19

Note. The background map is the curtsey of ©Google Earth.

20

21

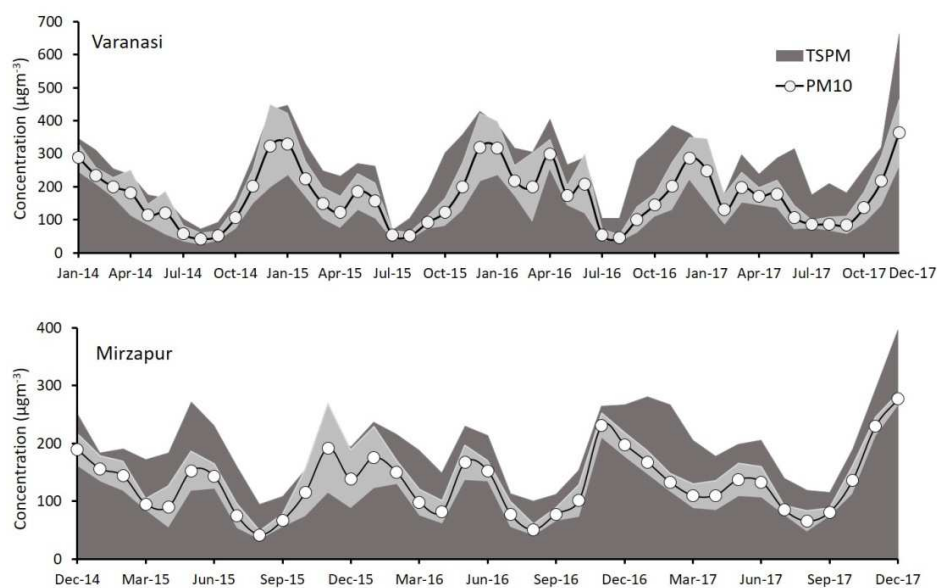


Figure 2. Monthly mean variations of airborne PM_{10} and total particulate mass concentrations.

Note. The dark shade indicate concentration of total particulate mass (TSPM) and light grey indicates the standard deviation of PM_{10} concentration.

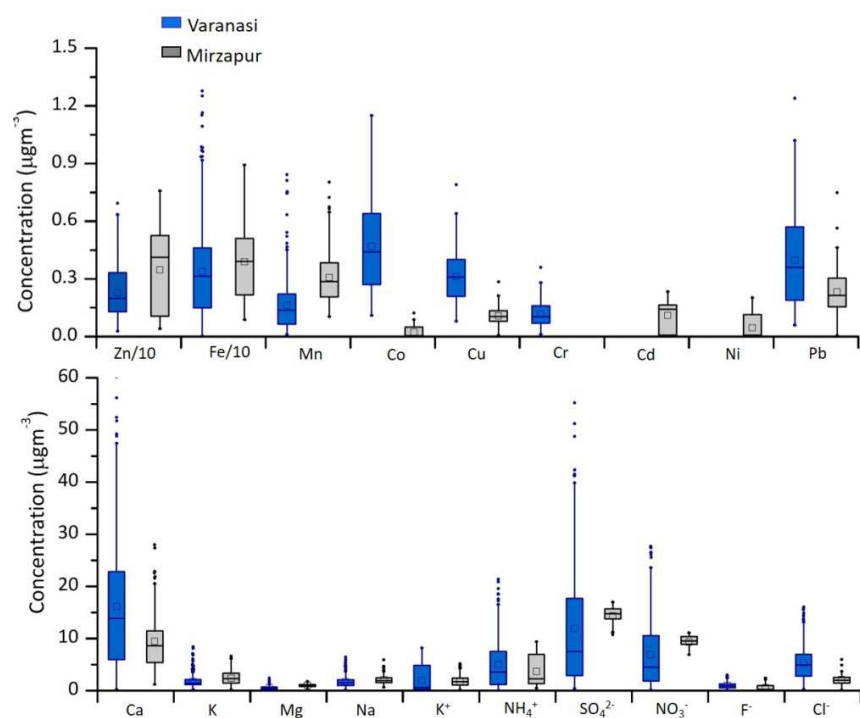


Figure 3. Distribution of particulate-bound elements and water-soluble ion concentrations.

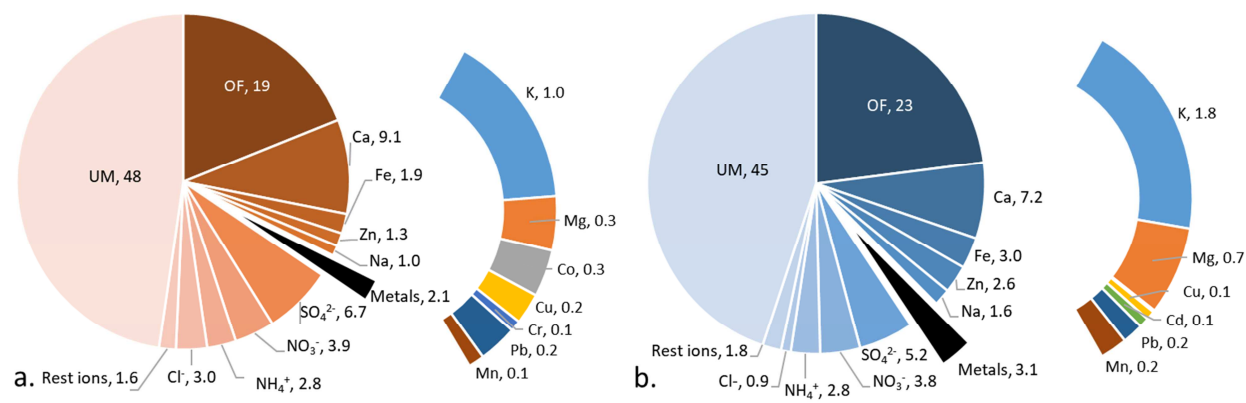


Figure 4. Relative composition of particulate in (a) Varanasi and (b) Mirzapur.

Note. Composition of rest of the trace metals (in black shade) are also classified. All unit are in percentage and the values represent overall mean contribution. UM- Unmeasured; OF- Organic fraction.

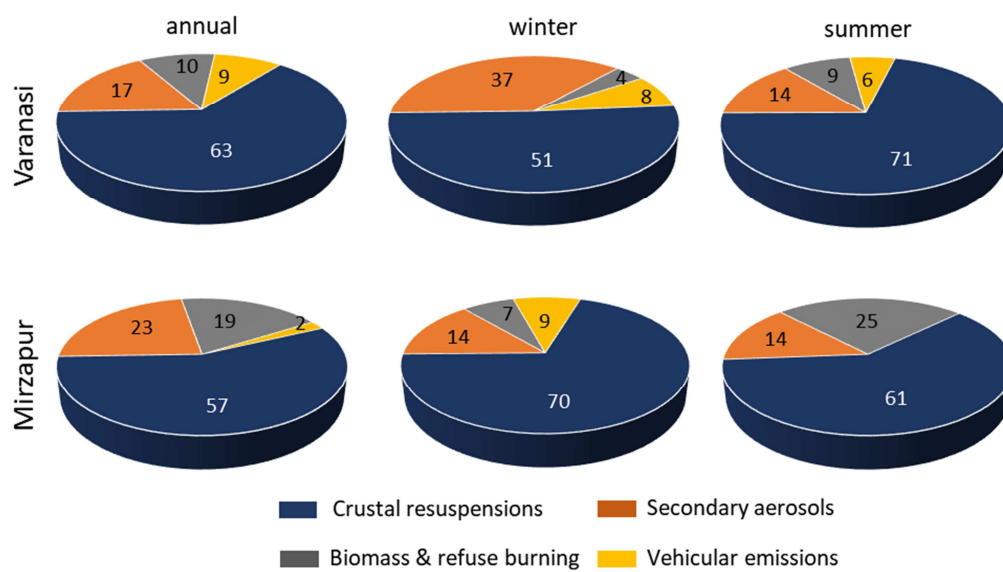


Figure 5. Relative contribution of various sources to airborne particulates.

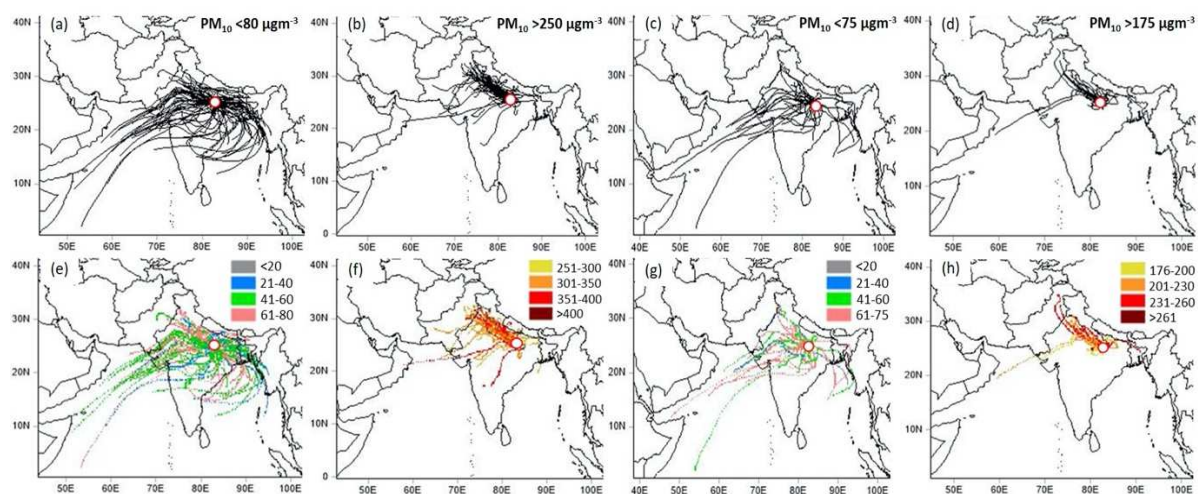


Figure 6. Potential particulate transport pathways (a-d) and source fields (e-h) during low and high PM_{10} loading conditions in Varanasi (a,b,e,f) and Mirzapur (c,d,g,h).

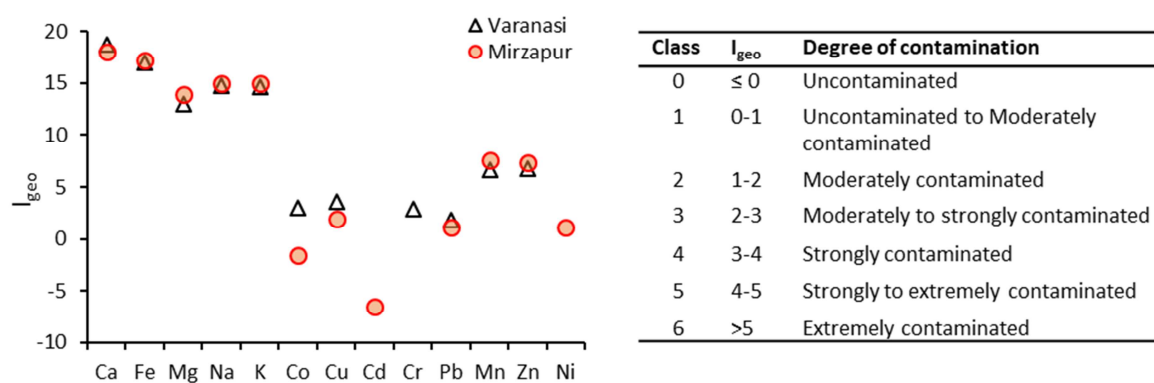


Figure 7. Geo-accumulation index of PM₁₀ bound metals and associated level of contamination.

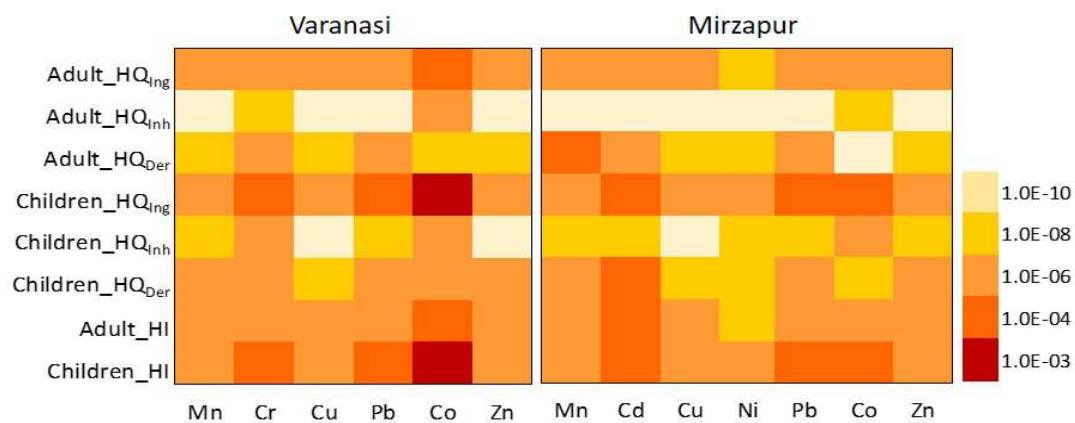


Figure 8. Hazard Quotient (HQ) and Hazard Index (HI) for adults and children with respect to PM₁₀ bound metal exposure.

Source apportionment and health risk assessment of airborne particulates over central Indo-Gangetic Plain

RESEARCH HIGHLIGHTS

- PM₁₀ concentration is very high over central Gangetic Plain, particularly in winter.
- Particulate bound elemental species are mostly of crustal origin.
- Secondary inorganic aerosols contribute 60% of total ionic load.
- Crustal resuspensions are most dominating source followed by secondary aerosols.
- Health-risk assessment concludes possible risk of contamination by Cr and Cd.

Source apportionment and health risk assessment of airborne particulates over central Indo-Gangetic Plain

Vishnu Murari¹, Nandita Singh¹, Rohit Ranjan², RS Singh³ and Tirthankar Banerjee^{1,2*}

¹Institute of Environment and Sustainable Development, Banaras Hindu University, Varanasi, India

²DST-Mahamana Centre of Excellence in Climate Change Research, Banaras Hindu University, Varanasi, India

³Department of Chemical Engineering and Technology, Indian Institute of Technology (BHU), Varanasi, India

*Correspondence: tb.iesd@bhu.ac.in; tirthankaronline@gmail.com

Competing interests. Authors declare that they have no conflict of interest.